PHILOSOPHICAL TRANSACTIONS OF THE ROYAL SOCIETY A MATHEMATICAL PHYSICAL & ENGINEERING SCIENCES

Characteristics and causes of shallow seismicity in andesite volcanoes

Jürgen Neuberg

Phil. Trans. R. Soc. Lond. A 2000 **358**, 1533-1546
doi: 10.1098/rsta.2000.0602

THE ROYAL SOCIETY

Characteristics and causes of shallow seismicity in andesite volcanoes

By Jürgen Neuberg

School of Earth Sciences, University of Leeds, Leeds LS2 9JT, UK

Recent observations from Soufrière Hills volcano in Montserrat reveal a wide variety of seismic signals. We focus here on characteristics of long-period events, and their role in the pressurization of the volcanic plumbing system. These events can occur in swarms and merge into tremor, an observation that sheds further light on the generation and composition of harmonic tremor. A two-dimensional finite-difference method has been employed to model major features of low-frequency seismic signatures and compare them with the observations. A depth-dependent seismic velocity model for a fluid-filled conduit is used that accounts for the varying gas content in the magma. We analyse episodes of tremor that show shifting spectral lines and model those in terms of changes in excess pressure due to unloading and degassing events. Potential trigger mechanisms are suggested and discussed.

Keywords: conduit resonance; tremor; long-period earthquake; pressurization

1. Introduction

Soufrière Hills volcano in Montserrat and many other volcanoes show a wide variety of seismic signals, but only low-frequency seismic events turn out to play a major role in any attempt to assess the eruptive stage of volcanic activity. These seismic signals have a frequency content ranging from 0.2 Hz to 5 Hz and show several unique features that make them indicative tools. Those features comprise

(i) the occurrence in swarms of earthquakes that precede volcanic eruptions (Lahr *et al*. 1994; Miller *et al*. 1998);

(ii) their close relationship to volcanic tremor with peaked spectral amplitudes; and

(iii) the fact that these swarms correlate well with tilt signals pointing to a pressurization of the volcanic plumbing system (Chouet *et al*. 1994; Voight *et al*. 1998; Neuberg *et al*. 1998).

For Montserrat, however, they cannot be related to the actual dome growth or changes in its rate in any simple causal way (Miller *et al*. 1998).

The seismic wavefield of low-frequency events is generated at the boundary between a fluid, i.e. magma, and a solid, i.e. the country rock, in the form of interface waves that allow seismic energy, generated and trapped in the fluid, to leak into, and propagate through, the solid medium. When such seismic signals are observed at the

surface they show a complicated interference pattern of waves originating from various parts of the magma-filled conduit, interacting with the free surface and interfaces in the volcanic edifice. Simple resonator models for volcanic tremor (see, for example, Hurst 1992; Seidl *et al.* 1981) based on point sources are, therefore, inadequate to describe such a wavefield. The characteristics of the wavefield are controlled by the contrast of elastic parameters across the interface, as well as the width of the conduit compared with the seismic wavelength. Therefore, it is crucial for the interpretation of the seismic signals to understand the behaviour of the elastic parameters in various parts of the conduit, particularly in the presence of gas.

A brief overview about the different types of seismic signals typically found on andesite volcanoes is presented in § 2. We then focus on low-frequency events and describe several characteristic features in § 3, before we model some of these features in § 4. After the wave generation and propagation have been examined we speculate about several trigger mechanisms and discuss their applicability in the last § 5.

2. General characteristics of seismicity

Descriptions of the volcano-seismic signals encountered on Montserrat can be found in Miller *et al.* (1998) and Aspinall *et al.* (1998). Here we focus on some special aspects of low-frequency seismic signals.

Volcano-tectonic events are 'normal' tectonic earthquakes due to brittle fracture. The fact that they occur underneath volcanoes points to changes in the stress field generated by rising magma in the early stages of an eruption, as well as during relaxation phases in later stages. They are easily recognized by their high-frequency content and show the separate arrivals of P-waves and S-waves if the travel path to the seismic station is long enough to allow separation.

An example of a seismic event with longer duration, cigar-shaped envelope and frequencies in the range 1–10 Hz can be seen in figure 1 (top trace). These correlate visually with avalanches of material from the lava dome and are referred to as *rockfall events*. These events can be used to determine the propagation direction of pyroclastic flows valuable at night or in conditions of poor visibility, and their characteristics, such as amplitude and duration, can give a vague estimate about the current stability of the lava dome.

Following Lahr *et al.* (1994), the *low-frequency events* have been subdivided into two families, *long-period (LP) earthquakes* and *hybrid earthquakes*, examples of which can be found in figure 1. These two types of event, however, are very similar and share common source processes; thus, a continuum exists between these idealized end-members. Long-period events are emergent and have monochromatic waveforms with a duration of several seconds. Their dominant frequency varies between 0.7 and 2.0 Hz. Hybrid events have, in addition, higher frequency components and sometimes impulsive onsets. The longest-lasting hybrid earthquakes have durations of a few tens of seconds. Spectral bandwidths of 0.5–4 Hz are typical. It was suggested in Neuberg *et al.* (1998) that the proportion of high-frequency energy in hybrid earthquakes is an indication of the depth at which they are triggered. The low-frequency part is typical for interface waves generated at the boundary of a fluid-filled conduit and surrounding rock. Low-frequency signals will be modelled in § 4.

A further signal type consists of a rockfall signal with a well-developed long-period precursor. We refer to such events as *long-period rockfalls*. The LP part of the signal

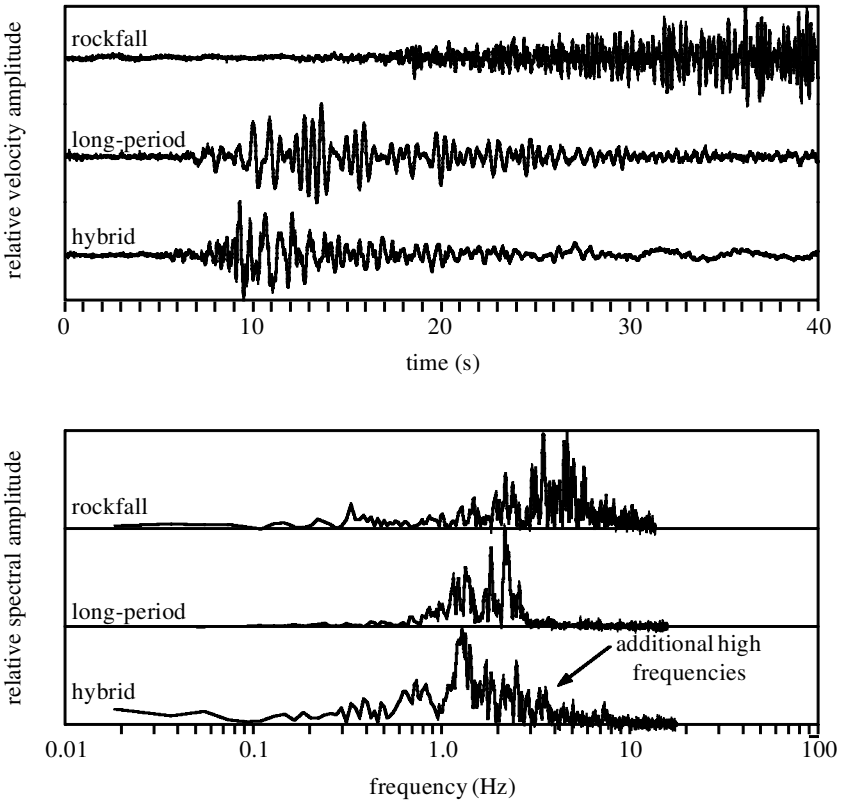

Figure 1. Comparison between an onset of rockfall signal and two low-frequency events. While the rockfall is dominated by high frequencies, the low-frequency events differ only in the amount of high frequencies for the hybrid, as indicated in the spectrum. Observations from Montserrat, station MBGA, vertical component, 25/6/97.

typically begins 10–20 s before the start of the rockfall. This has been confirmed by using a GPS-synchronized video camera to record the rockfall activity. It has been suggested that the seismic energy concentrated within the dome structure (Neuberg *et al*. 2000) leads to a destabilization of the dome and rockfall.

In the sections that follow, we focus on the *low-frequency events* without distinguishing between hybrids and LPs. The following characteristic features that have been observed provide important clues about the excitation mechanism and seismo-volcanic source processes.

3. Characteristic features of low-frequency events

(*a*) *Swarms and tremor*

Low-frequency earthquakes on Montserrat have, in general, occurred in swarms lasting between a few hours and several days. Almost all large collapses from the growing lava dome were preceded by swarms of low-frequency earthquakes (figure 2). Swarms were often periodic and occurred every 8–12 h for several weeks. At times, this periodicity correlates with tilt measurements made on the volcano, which indicates that

the dome inflates during a swarm and deflates when it finishes; this last change often being associated with dome collapse and pyroclastic flows (Voight *et al.* 1998). For most swarms in 1996 the individual earthquakes were very similar to each other in both amplitude and waveform, having cross-correlation coefficients of 0.9 ± 0.1 (White *et al.* 1998). During a swarm, events can occur at very regular intervals, with the time between consecutive events varying by less than 2% for several hours on end (White *et al.* 1998). Given the similarity of the waveforms, that observation points to a repeatable, non-destructive source mechanism at a fixed source location. Occasionally, individual events become closer and closer together in time until they merge into continuous tremor (figure 2). For single events and tremors alike, the spectra are not coherent over the array and it is not possible to distinguish between path effects and source effects.

(*b*) *Peaked spectra*

In a few cases, however, there are intervals of several minutes within a tremor episode, when one fundamental frequency and a varying number of its harmonic overtones dominate the signals at every station. For each occurrence the frequencies concerned are different, and, in several cases, the frequencies shift within a given episode (figure 5). During these intervals of coherence across the array the amplitude of the tremor changes, in some cases increasing and in others decreasing. This type of harmonic tremor with shifting dominant frequencies has been observed on many other volcanoes—such as Langila (Mori *et al.* 1989), Semeru (Schlindwein *et al.* 1995), and Arenal (Benoit & McNutt 1997)—and has been interpreted in almost as many ways.

Peaked spectra can be produced in two ways:

(i) by a repetitive triggering of an identical source wavelet where the fundamental frequency and its harmonics are controlled by the triggering mechanism, and the relative amplitudes of these peaks are determined by the shape of the spectrum of the source wavelet (Schlindwein *et al.* 1995); or, alternatively,

(ii) a peaked spectrum depicts the eigenfrequencies of a resonating system and the shifting of these frequencies implies changes in the parameter set that controls the eigenoscillations (Benoit & McNutt 1997).

In § 5 we will come back to a discussion on both of these interpretations, once some resonance models have shed further light on the possible generation of low-frequency seismic signals.

(*c*) *Observational clues*

In the following we list the constraints that are provided by the interpretation of the characteristic features described above. These constraints must be taken into account whenever an attempt is made to forward model seismo-volcanic processes.

(1) The high similarity of repeated LP waveforms points to a common excitation mechanism at a source location, fixed within a volume with dimensions not more than a few hundred metres.

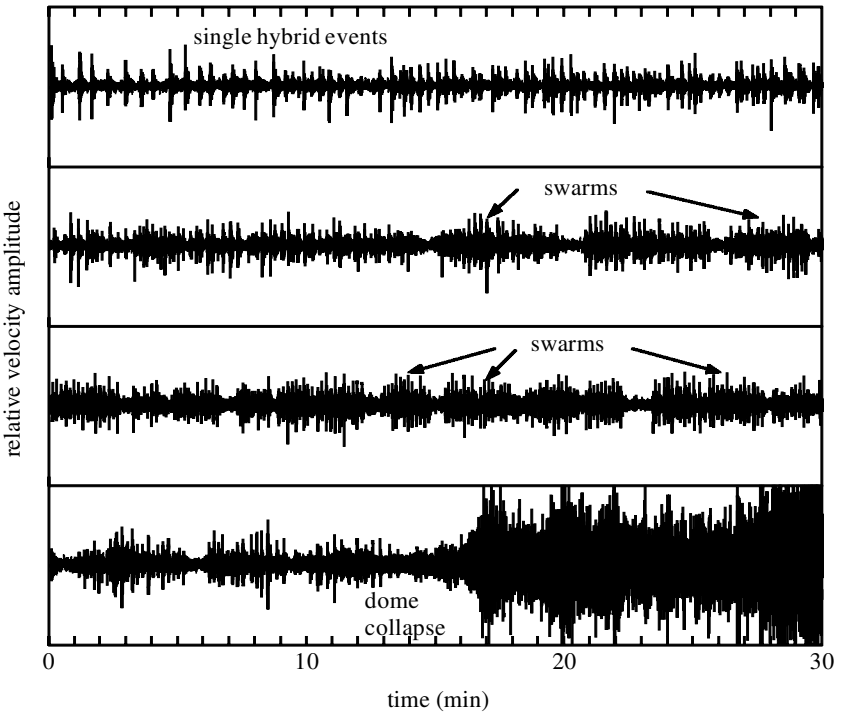

Figure 2. Single hybrid events merge into distinct swarms and, a short time before a dome collapse, into tremor. Observations from Montserrat, station MBGA, vertical component, 25/6/97.

(2) The regular occurrence of LPs within swarms indicates highly periodic excitation by a repeatable non-destructive stationary source.

(3) The merging of LPs into tremor explains some examples of harmonic tremor as a superposition of single seismic events.

(4) The correlation between LP swarms and inflating tilt qualitatively suggests a link to the pressurization of the upper part of the volcanic edifice.

(5) The dominance of low-frequency energy in the seismic signature of LPs and hybrids points to the generation of interface waves at the boundary of a fluid embedded in a solid.

4. Forward modelling: conduit resonance

(*a*) *Model*

A finite-difference code for modelling a magma-filled conduit embedded in an elastic medium is employed to generate the seismic wavefield in and around the conduit. The code solves the two-dimensional elastic equations of motion (Levander 1988) using a 4th-order staggered-grid method. We chose a discrete grid spacing of 2 m corresponding to approximately 25 points per minimum wavelength of 50 m. Absorbing boundary conditions at the sides have been used and an attenuative zone of exponential damping has been incorporated along a 35 grid-point region to limit reflections

Table 1. *Conduit parameters*

density of country rock (kg m^{-3})	2600
density of gas-free magma (kg m^{-3})	2300
P-wave velocity in country rock (m s^{-1})	3000
P-wave velocity in gas-free magma (m s^{-1})	1400
S-wave velocity in country rock (m s^{-1})	1725
S-wave velocity in gas-free magma (m s^{-1})	0
conduit dimensions (width × length) (m^2)	20×2000
conduit temperature (°C)	1200
excess pressure (MPa)	3–9
gas mass fraction $H_2 0$ (%)	1–5

from model boundaries (Cerjan *et al.* 1985). The seismograms are 'observed' at the stress-free boundary. The model is closed in the sense that the fluid in the conduit does not reach the surface. The time increment used in the finite-difference code is fixed at 0.0002 s. All model parameters used in the computation are listed in table 1.

The aim of such a modelling procedure is to determine the sensitivity of results to the influence of each independent parameter, and this is why a physical model must be kept simple. Incorporating too much complexity in the model with the intention of achieving a high degree of reality often defeats such a purpose. Here, we concentrate on the impact of variations of elastic parameters across the interface between conduit and elastic rock (impedance contrast) where the seismic signals are generated. The variations in these parameters are controlled by the gas content as a function of depth.

(*b*) *Depth-dependent seismic velocity*

A steady homogeneous magma model is used to derive the relationships between gas mass and volume fraction, density, temperature and pressure as a function of depth. These parameters are then used to obtain the vertical seismic velocity profile in the gas-charged magma.

The depth-dependent pressure is given by

$$P(z) = P_{\mathrm{ex}} + \int_0^z g\rho(z')\,\mathrm{d}z', \tag{4.1}$$

where P_{ex} is the excess pressure, g is the acceleration due to gravity, and $\rho(z)$ is the bulk density of the gas–liquid mixture.

In a fixed volume at depth z the fractions of gas and liquid are given by

$$\frac{1}{\rho(z)} = \frac{1-n_{\mathrm{g}}}{\rho_{\mathrm{l}}} + \frac{n_{\mathrm{g}}}{\rho_{\mathrm{g}}(z)}, \tag{4.2}$$

where ρ_{l} is the (constant) density of liquid magma, ρ_{g} the density of gas, and n_{g} the gas mass fraction. The gas density is obviously pressure dependent, and, therefore, depth dependent, and is controlled by the gas law

$$\rho_{\mathrm{g}}(z) = mP(z)/RT, \tag{4.3}$$

with R being the gas constant, m the molecular mass of the relevant gas (SO_2 or H_2O), and T the magma temperature.

If n_{total} is the total volatile mass fraction of exsolved and dissolved gas, the amount of exsolved gas affecting the elastic properties of the magma is described by the solubility law (Shaw 1974)

$$n_{\mathrm{g}} = n_{\mathrm{total}} - s\sqrt{P(z)}, \tag{4.4}$$

where the constant $s = 4.1\times10^{-6}$ Pa$^{-1/2}$ was calibrated experimentally on a rhyolitic liquid with water as the only volatile in the system.

For the determination of the seismic properties in the gas–liquid mixture the relevant parameter is the volume fraction occupied by the gas, m_{g}, rather than its mass fraction. With M, M_{g}, V and V_{g} denoting mass and volume of mixture and gas, respectively, $M_{\mathrm{g}} = V_{\mathrm{g}}\rho_{\mathrm{g}}$, and, therefore, $n_{\mathrm{g}}M = m_{\mathrm{g}}V\rho_{\mathrm{g}}$. The gas volume fraction, m_{g}, can be easily derived from the mass fraction n_{g}, weighted by the ratio of bulk and liquid density:

$$m_{\mathrm{g}} = (\rho/\rho_{\mathrm{g}})n_{\mathrm{g}}. \tag{4.5}$$

We use an iterative approach and start at the (linear) lithostatic pressure profile and work out gas content and densities, which are used in further iterations to determine the depth-dependent pressure in equation (4.1). The seismic (acoustic) velocity in the gas-charged magma is given by

$$\alpha = \sqrt{B/\rho}, \tag{4.6}$$

where B is the bulk modulus of the magma representing its incompressibility or resistance to a pressure change dP. With the gas volume $V_{\mathrm{g}} = m_{\mathrm{g}}V$ and the liquid volume $V_{\mathrm{l}} = (1 - m_{\mathrm{g}})V$ we obtain for the bulk modulus of the mixture:

$$\frac{1}{B} = \frac{(1 - m_{\mathrm{g}})}{B_{\mathrm{l}}} + \frac{m_{\mathrm{g}}}{B_{\mathrm{g}}}. \tag{4.7}$$

With equation (4.5) we replace the gas volume fraction m_{g} by the gas mass fraction n_{g} and obtain

$$\frac{1}{B} = \frac{\rho}{B_{\mathrm{l}}\rho_{\mathrm{l}}}(1 - n_{\mathrm{g}}) + \frac{\rho}{B_{\mathrm{g}}\rho_{\mathrm{g}}}n_{\mathrm{g}}, \tag{4.8}$$

and by multiplying by ρ and taking the square root we obtain the inverse acoustic velocity $1/\alpha$

$$\sqrt{\frac{\rho}{B}} = \sqrt{\frac{\rho^2}{B_{\mathrm{l}}\rho_{\mathrm{l}}}(1 - n_{\mathrm{g}}) + \frac{\rho^2}{B_{\mathrm{g}}\rho_{\mathrm{g}}}n_{\mathrm{g}}}, \tag{4.9}$$

and, therefore,

$$\alpha = 1\Big/\left(\sqrt{\frac{\rho^2}{B_{\mathrm{l}}\rho_{\mathrm{l}}}(1 - n_{\mathrm{g}}) + \frac{\rho^2}{B_{\mathrm{g}}\rho_{\mathrm{g}}}n_{\mathrm{g}}}\right). \tag{4.10}$$

The seismic velocity and the bulk density in the conduit can now be evaluated at any depth as a function of excess pressure and gas content (figure 3), and can be

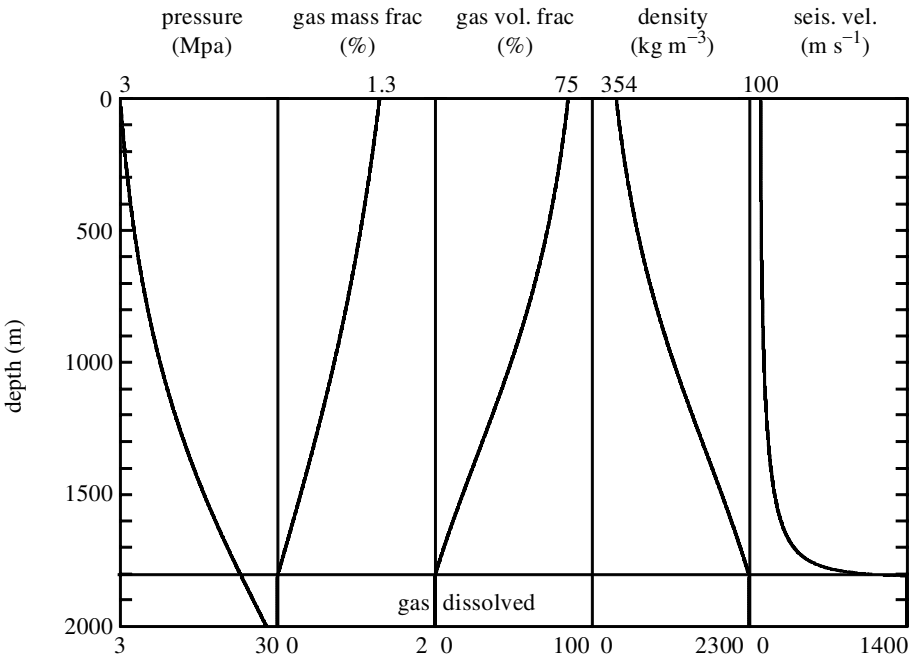

Figure 3. Conduit parameters for a magma model of 2% total water content. Parameter ranges are indicated at the bottom, values for the upper end of the conduit at the top. At vesiculation level the seismic velocity decreases rapidly to values as small as 100 m s^{-1}.

compared with the corresponding quantities in the surrounding rock. Their contrast across the conduit wall, together with the ratio between seismic wavelength and conduit diameter, control the properties of the seismic wavefield that is radiated from such a structure.

(*c*) *Trapped waves*

The low-frequency content of these seismic signals is indicative of the existence of interface waves generated at a fluid–elastic boundary. Those waves were first found near fluid-filled boreholes and identified as tube-waves by Biot (1952). Aki *et al.* (1977) linked them to volcanic signals in their fluid-driven crack models. Latter (1979) suggested that, for Mount Ruapehu, single low-frequency events and tremor share the same source, an idea later confirmed by Fehler (1983), who pointed out the spectral similarities between tremor and single events. Chouet continued the pioneering work by Aki *et al.* (1977) in a series of contributions (see, for example, Chouet 1986, 1988), where he modelled fluid-filled cracks and compared what he called 'crack waves' with seismic observations. Ferrazzini & Aki (1987) followed an elegant analytical approach and derived the dispersion relation of what they called 'slow waves'. The so-called stiffness factor,

$$C = BL/\mu h, \tag{4.11}$$

was introduced by Aki *et al.* (1977) and summarizes the controlling parameters, where B is the bulk modulus of the fluid, L the length of the conduit, μ the rigidity of the elastic medium, and h the conduit width.

An explosive source in the fluid produces P-waves, only a small fraction of which can leave the conduit directly. Given an impedance contrast of $\alpha_m \rho_m / \alpha\rho = 2.5$, where α_m and ρ_m are the seismic velocity and density of the elastic medium surrounding the conduit, we obtain a critical angle of reflection $i_{crit} = \arcsin(\alpha/\alpha_m) = 30°$, i.e. most of the energy is reflected at the interface, and beyond the critical angle converted into inhomogeneous waves of the type

$$u_{x/z} = u_0 e^{-k_x|x|}(e^{ik_z z} + e^{-ik_z z})e^{i\omega t}. \tag{4.12}$$

This set of inhomogeneous waves propagating up and down the conduit walls form the low-frequency wavefield that leaks energy into the elastic medium. Whatever source mechanism might trigger a pressure perturbation in the magma, the generation of the actual seismic wavefield happens along the conduit walls in the same way as (low-frequency) surface waves are generated by earthquake sources.

The higher the impedance contrast across the conduit walls, the more effective is the entrapment of seismic energy, leading to a long-lived conduit resonance. This mechanism is fundamentally different from a resonating (fluid-filled) body with corresponding eigenfrequencies (so-called 'organ-pipe modes'; see Schlindwein *et al.* (1995)), as their resonant behaviour is merely based on the acoustic velocity of the body rather than on the interaction between fluid and elastic medium.

Even brittle fracture in the rock surrounding a fluid-filled conduit can produce resonances once some of the seismic energy enters the fluid and is trapped there. In this case, the corresponding seismic wavefield will have high-frequency components originating from the rock fracture and low-frequency components from the subsequent resonance, and, hence, produces the combination of frequency contents observed in hybrid events.

(*d*) *Modelling results*

With the finite-difference method introduced in § 4 *a* and the velocity–density model described in § 4 *b* we have studied the impact of several parameters on the seismic wavefield by varying source depth, conduit dimensions, gas content and excess pressure. Figure 4 shows an example of a synthetic seismogram 'recorded' at the surface at an epicentral distance of 500 m, as well as four 'snapshots' of the seismic wavefield after 1, 8, 12 and 17 s, respectively. The signal is triggered by an initial pressure drop at shallow depth simulating a sudden degassing event or ash venting.

(i) *Wavefield snapshots*

This seismogram example has been chosen because it shows several features that match observations. While most of the seismic energy is trapped in the conduit, there is, at $t = 1$ s, an initial, weak P-wave visible, followed immediately by high-amplitude interface waves. This P-wave, which shows a longitudinal particle motion for not longer than half a wavelength, is very important as it can be used to determine the source location of the seismic trigger. In the next few seconds a resonance pattern develops which is dominated by small-amplitude monochromatic pulses whose wavefronts detach themselves from the conduit and propagate through the medium. After 12 s the slow wavefront in the gas-rich magma has reached the vesiculation level (1800 m depth, figure 3), where the impedance contrast across the conduit wall

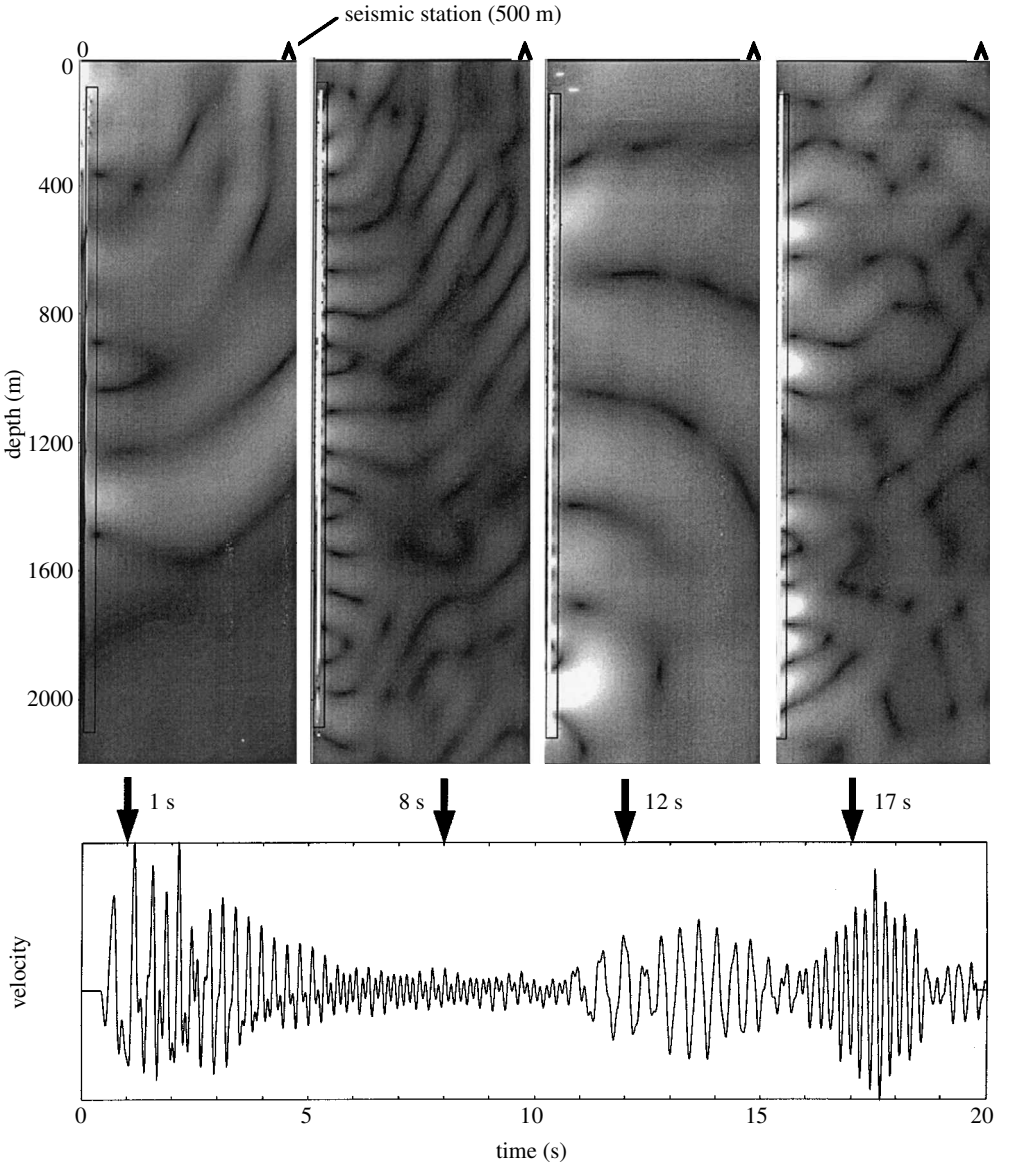

Figure 4. Two-dimensional snapshots of the wavefield radiated from different parts of a vertical conduit (indicated at the left), conduit model: figure 3. The synthetic seismogram shows distinct phases during the conduit resonance.

decreases drastically. Much more energy leaks into the elastic medium and several wavefronts (with a lower-frequency content) are radiated from the lower end of the conduit. At the seismic station these pulses appear to be a secondary phase arrival. After 17 s a stable resonance pattern has been established producing an additional wave group. The extremely short P-wave, the highly periodic resonance signature as well as the distinct later phase arrivals are features that closely match the observations.

(ii) *Gliding spectral lines*

In a next step we simulate the characteristic spectral shift of volcanic tremor as discussed in § 3 *b*. The system in the following model is only triggered once, but the elastic parameters of the fluid are varied with time. Within the event duration being considered, it is impossible for the magma to degas internally to such an extent that the elastic parameters would be significantly affected. Therefore, in this model the gas content is fixed at 5% and the excess pressure now drops from 5 MPa to 3 MPa. This simulates, for example, the release of pressure caused by a longer episode of ash venting. The pressure drop has only a minimal effect on the velocity profile of the conduit, the difference in velocity values being only 5 m s^{-1} in places. However, this change is enough to cause a slight shift in the spectral peaks, more so at the higher frequencies. This is in good agreement with observations from Montserrat and elsewhere, and demonstrates that amongst conduit parameters, a pressure change is the most likely candidate for a physical process that can lead to gliding spectral lines. The spectrogram in figure 5, for instance, can then be interpreted in terms of a pressure increase by several MPa, followed by an explosion.

Further modelling results include examples of long-lived resonances lasting for several tens of seconds when the impedance contrast is high enough to trap seismic energy efficiently. However, a repetitive trigger is necessary to produce swarms such as those depicted in figure 2. If a repetitive source triggers individual events in short time-intervals, such that their seismic signals overlap and merge into tremor, a peaked spectrum with integer harmonic overtones will be observed. In this case, shifting spectral lines would indicate the change in the triggering frequency of the source and figure 5 could then be interpreted in terms of an increasing number of triggered events leading to the explosion.

5. Speculations and discussion on trigger mechanisms

While the generation and propagation of the long-period seismic wavefield is well understood, the actual trigger mechanism that kick-starts conduit resonances in the first place is still a subject of speculation. Taking the observational constraints of § 3 into account, the main criterion that any source mechanism must satisfy is the ability to act repeatedly and, essentially, non-destructively.

Hellweg (2000) suggests so-called *eddy shedding* as a source mechanism, where eddies that regularly form behind an obstacle act as sources of pressure fluctuations. Such a source could act repeatedly and would be stationary, but the flow conditions necessary for eddy shedding are not satisfied for andesite magmas, where the flow velocity is too low and viscosity too high. Johnson & Lees (2000) suggest a periodic ash release in their *pressure-cooker model*, a concept very similar to Hellweg's (2000) *soda-bottle model*. In both cases, periodic degassing is invoked in which some 'valve mechanism' controls the periodicity. While these models could explain the ash-venting episodes, sometimes referred to as *chugging* (Benoit & McNutt 1997), the shallow source location is not consistent with observations on Montserrat, where sources determined by P-waves are in a depth range of 1000–3000 m.

Spines on Soufrière Hills in 1996 appeared to have *watermarks* on them, suggesting that they had moved up in a *stick-slip* manner, and attempts were being made to correlate the biggest LPs with movements of various spines (W. P. Aspinall, personal communication, 1999). Also S. D. Malone (personal communication, 1999) proposes a

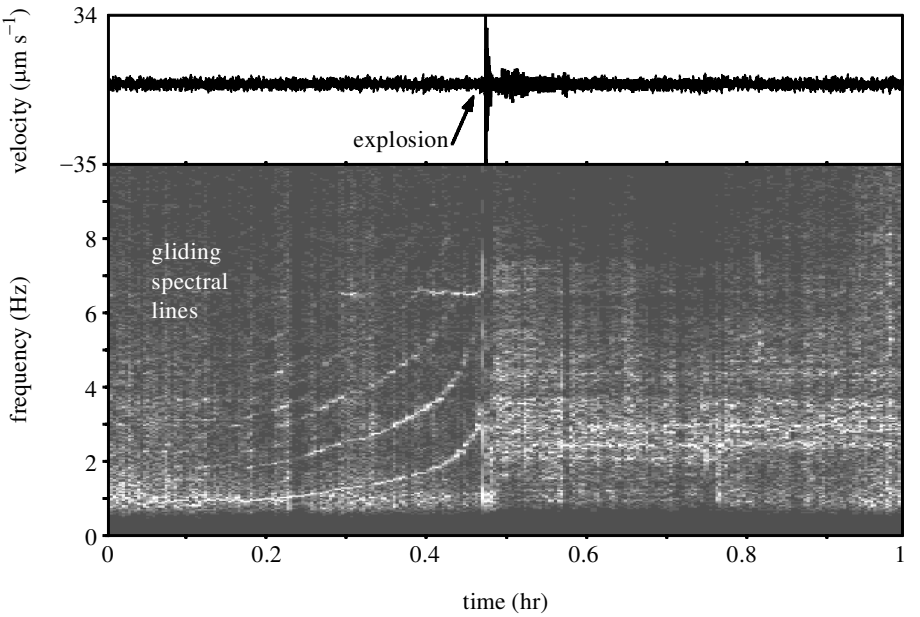

Figure 5. Gliding spectral lines prior to an explosion. This feature can be interpreted in terms of increasing pressure in the conduit, or an increasing repetition rate for hybrid source triggers preceding the explosion. Observation from Montserrat, station MBRY, 7/1/99.

partial stick-slip flow mechanism, where very viscous magma can sustain shear stress until brittle failure occurs. Such a system could provide effective seismic sources, but the coexistense of very viscous magma to provide the trigger at depth and a fluid to allow for the generation of low-frequency events is still to be investigated further.

G. R. Robson (personal communication, 1997) suggested *magma–water interaction* as a non-destructive source mechanism. Premixing of sea, rain or ground water with magmatic melt can lead to phreatomagmatic explosions when the mixture, in a stable condition, experiences a pressure perturbation such as might be generated by a variety of volcano-seismic signals (Zimanowski 1998). At a depth of 2000 m, the high lithostatic pressure would prevent magma fragmentation, but an interaction between water and magmatic melt might still set off a small phreatomagmatic explosion, triggering a seismic low-frequency event. Once the magma–water system is recharged, a resonating seismic signal could set off the next explosion, leading to a feedback mechanism. This (admittedly highly speculative) model could, however, simultaneously explain the occurrence of LP swarms, single events initially widely spaced and merging into tremor, and could provide a link between a prolonged conduit resonance and repeated triggering of low-frequency events as well.

6. Conclusions

The discussion above makes it clear that the question over possible trigger mechanisms for long-period events is a key issue for the understanding and interpretation of seismicity as a diagnostic tool. It is also certain that further progress depends on a multidisciplinary approach whereby seismic models are better guided by geochem-

ical and petrological constraints. As to the interpretation of seismicity in andesite volcanoes, to date we draw the following conclusions.

(1) Appropriately analysed seismic signals can reveal the source location and source processes of volcanic activity.

(2) Low-frequency events indicate a 'charging mechanism'.

(3) Seismic signals from rockfall events can give an indication of on-dome instability and information on the direction of pyroclastic flows.

(4) Single low-frequency events can be triggered by unloading or sudden decompression.

(5) Swarms of low-frequency events require a repetitive, non-destructive, stationary source mechanism.

(6) Gliding spectral lines indicate either pressure changes in the magmatic system or changes in the rate of excitation trigger mechanisms.

Most of this work has been done in cooperation with Brian Baptie and Richard Luckett, both British Geological Survey (BGS), as well as Clare O'Gorman, University of Leeds. I thank Lionel Wilson for many interesting and enjoyable discussions on the physics of magma, and Kim Olsen for supporting the FD calculations. The constructive review by Willy Aspinall did much to improve the manuscript. Many thanks to the staff of the Montserrat Volcano Observatory (MVO) for providing the seismic data and their general assistance. The MVO is supported by the Department for International Development (UK) and the BGS.

References

Aki, K., Fehler, M. & Das S. 1977 Source mechanism of volcanic tremor: fluid-driven crack models and their application to the 1963 Kilauea eruption. *J. Volcanol. Geotherm. Res.* **2**, 259–287.

Aspinall, W. P., Miller, A. D., Lynch, L. L., Latchman, J. L., Stewart, R. C., White, R. A. & Power, J. A. 1998 Soufrière Hills eruption, Montserrat, 1995–1997: volcanic earthquake locations and fault plane solutions. *Geophys. Res. Lett.* **25**, 3397–3400.

Benoit, J. & McNutt, S. 1997 New constraints on source processes of volcanic tremor at Arenal Volcano, Costa Rica, using broadband seismic data. *Geophys. Res. Lett.* **24**, 449–452.

Biot, M. A. 1952 Propagation of elastic waves in a cylindrical bore containing a fluid. *J. Appl. Phys.* **42**, 82–92.

Cerjan, C., Kosloff, D., Kosloff, R. & Reshef, M. 1985 A nonreflecting boundary condition for discrete acoustic and elastic wave equations. *Geophys.* **50**, 705–708.

Chouet, B. A. 1986 Dynamics of a fluid-driven crack in three dimensions by the finite difference method. *J. Geophys. Res.* **91**, 13 967–13 992.

Chouet, B. A. 1988 Resonance of a fluid-driven crack: radiation properties and implications for the source of long-period events and harmonic tremor. *J. Geophys. Res.* **93**, 4373–4400.

Chouet, B. A., Page, R. A., Stephens, C. D., Lahr, J. C. & Power, J. A. 1994 Precursory swarms of long-period events at Redoubt Volcano (1989–1990), Alaska: their origin and use as a forecasting tool. *J. Volcan. Geotherm. Res.* **62**, 95–135.

Fehler, M. C. 1983 Observation of volcanic tremor at Mount St. Helens volcano. *J. Geophys. Res.* **88**, 3476–3484.

Ferrazzini, V. & Aki, K. 1987 Slow waves trapped in a fluid-filled infinite crack: implication for volcanic tremor. *J. Geophys. Res.* **92**, 9215–9223.

Hellweg, M. 2000 Physical models for the source of Lascar's harmonic tremor. *J. Volcanol. Geotherm. Res.* (In the press.)

Hurst, A. W. 1992 Stochastic simulation of volcanic tremor from Ruapehu. *J. Volcan. Geotherm. Res.* **51**, 185–198.

Johnson, J. B. & Lees, J. M. 2000 Plugs and chugs—strombolian activity at Karymsky, Russia and Sangay, Ecuador. *J. Volcanol. Geotherm. Res.* (In the press.)

Lahr, J., Chouet, C., Stephens, C., Power, J. & Page, R. 1994 Earthquake classification, location and error analysis in a volcanic environment: implications for the magmatic system of the 1989–1990 eruptions at Redoubt Volcano, Alaska. *J. Volcanol. Geotherm. Res.* **62**, 137–151.

Latter, J. H. 1979 Volcanological observations at Tongariro National Park. 2. Types and classification of volcanic earthquakes 1976–1978. New Zealand Department of Scientific and Industrial Research, Geophysics Division, Wellington, New Zealand, report 150.

Levander, A. R. 1988 Fourth-order finite-difference P–SV seismograms. *Geophys.* **53**, 1425–1436.

Miller, A., Stewart, R., White, R., Luckett, R., Baptie, B., Aspinall, W., Latchman, J., Lynch, L. & Voight, B. 1998 Seismicity associated with dome growth and collapse at the Soufrière Hills volcano, Montserrat. *Geophys. Res. Lett.* **25**, 3401–3404.

Mori, J., Patia, H., McKee, C., Itikarai, C., Lowenstein, P., De Saint Ours, P. & Talai B. 1989 Seismicity associated with eruptive activity at Langila Volcano, Papua New Guinea. *J. Volcanol. Geotherm. Res.* **38**, 243–255.

Neuberg, J., Baptie, B., Luckett, R. & Stewart, R. 1998 Results from the broadband seismic network on Montserrat. *Geophys. Res. Lett.* **25**, 3661–3664.

Neuberg, J., Luckett, R., Baptie, B. & Olsen, K. B. 2000 Models of tremor and low-frequency earthquake swarms on Montserrat. *J. Volcanol. Geotherm. Res.* (In the press.)

Schlindwein, V., Wassermann, J. & Scherbaum F. 1995 Spectral analysis of harmonic tremor signals at Mt. Semeru volcano, Indonesia. *Geophys. Res. Lett.* **22**, 1685–1688.

Seidl, D., Schick, R. & Riuscetti, M. 1981 Volcanic tremors at Etna: a model of hydraulic origin. *Bull. Volcanol.* **44**, 43–56.

Shaw, H. R. 1974 Diffusion of H_2O in granitic liquids. Part I. Experimental data. Part II. Mass transfer in magma chambers. In *Geochemical transport and kinetics* (ed. A. W. Hofmann, B. J. Giletti, H. S. Yoder & R. A. Yund), vol. 634, pp. 139–170. Washington, DC: Carnegie Institute.

Voight, B., Hoblitt, R. P., Clarke, A. B., Lockhart, A. B., Miller, A. D., Lynch, L. & McMahon, J. 1998 Remarkable cyclic ground deformation monitored in real-time on Montserrat, and its use in eruption forecasting. *Geophys. Res. Lett.* **25**, 3405–3408.

White, R., Miller, A., Lynch, L., Power, J. & Montserrat Volcano Observatory Staff 1998 Observations of hybrid seismic events at Soufrière Hills volcano, Montserrat, West Indies: July 1995 to September 1996. *Geophys. Res. Lett.* **25**, 3657–3660.

Zimanowski, B. 1998 Phreatomagmatic explosions. In *From magma to tephra* (ed. A. Freundt & M. Rosi). Elsevier.